

# Sm–Co hard magnetic nanoparticles prepared by surfactant-assisted ball milling

Yiping Wang, Yang Li, Chuanbing Rong and J Ping Liu

Department of Physics, The University of Texas at Arlington, Arlington, TX 76019, USA

E-mail: [pliu@uta.edu](mailto:pliu@uta.edu)

Received 6 June 2007, in final form 7 September 2007

Published 12 October 2007

Online at [stacks.iop.org/Nano/18/465701](http://stacks.iop.org/Nano/18/465701)

## Abstract

Hard magnetic nanoparticles based on the  $\text{Sm}_2\text{Co}_{17}$  and  $\text{SmCo}_5$  systems have been successfully produced using a surfactant-assisted ball milling technique. A size-selection process has been developed to obtain nanoparticles of different sizes with narrow size distribution. Significant room-temperature coercivity up to 3.1 kOe has been achieved with the  $\text{Sm}_2\text{Co}_{17}$ -based nanoparticles of an average size of 23 nm. It has been found that surfactants play multifold roles in the processing.

(Some figures in this article are in colour only in the electronic version)

## 1. Introduction

Magnetic nanoparticles with high magnetocrystalline anisotropy such as FePt-based systems have drawn great attention because of their potential applications in high density magnetic recording [1] and high energy-product permanent magnets [2]. Rare-earth transition-metal compounds based on the  $\text{SmCo}_5$  and  $\text{Sm}_2\text{Co}_{17}$  systems have the highest magnetocrystalline anisotropy (up to  $20 \times 10^6 \text{ J m}^{-3}$ ) [3] among all the known materials and therefore are very attractive for the applications. Unfortunately, nanoparticles of the rare-earth-containing systems are very active and prone to oxidation in ambient condition and the preparation of monodisperse Sm–Co nanoparticles has been proved to be very difficult. Significant efforts have been made recently in the synthesis of Sm–Co nanoparticles [4–8]. However, no room-temperature coercivity of the produced Sm–Co nanoparticles has been reported, which indicates that the hard magnetic phases with high magnetocrystalline anisotropy may have not been formed.

Ball milling is a typical technique for preparation of powder particles in the metallurgical and ceramic industries. For metallic systems, usually microsize particles are obtained even for an extended milling time because the crushed fine particles can be cold welded again during ball milling [9]. Surfactant addition can improve the milling efficiency so that smaller particles down to nanoscale size can be obtained [10–13]. We have adopted a surfactant-assisted ball milling method to produce magnetic nanoparticles of

various compositions [14]. However, wide size distribution and particle contamination are still two major barriers *en route* for further applications of ball-milled magnetic nanoparticles. For instance, a ball-milled nanoparticle powder with average size of 25 nm can easily have a wide size distribution from a few nanometers to hundred nanometers [12]. Contamination and amorphization of fine particles during the milling process may be responsible for the loss of magnetic properties [14].

In this paper we report our recent results in size control of ball-milled Sm–Co nanoparticles. Based on a sophisticated control of the ‘settling-down’ time of the nanoparticle solutions and a proper use of centrifugal separation, a size-selection process has been developed.  $\text{Sm}_2\text{Co}_{17}$  nanoparticles with narrow size distributions and remarkable room-temperature magnetic properties have been successfully obtained.

## 2. Experiments

Two compositions of the Sm–Co systems,  $\text{SmCo}_5$  and  $\text{Sm}_2\text{Co}_{17}$ , both commercially available, have been studied in our experiments. The raw materials have particle sizes from  $\sim 10$  to  $45 \mu\text{m}$ . The organic solvent heptane (99.8% purity) was used as the milling medium and oleic acid (90%) and oleyl amine (98%) were used as the surfactants during milling. The powders were ground in a milling vial with balls made of 440C hardened steel by using a Spex 8000M high-energy ball milling machine. The milling process and handling of the starting

materials and the milled products were carried out in an argon gas environment inside a glove box to protect the particles from oxidation.

Samples for magnetic characterization were prepared by embedding the nanoparticles in epoxy inside a glove box. An alternating gradient magnetometer (AGM) was used for the magnetic measurements. Structural and morphological characterizations were made using x-ray diffraction (XRD), a transmission electron microscope (TEM), and energy dispersive x-ray (EDX) analysis.

### 3. Results and discussion

Systematic investigations on the milling process indicated that the amounts of the solvent and surfactants, which have direct effects on the viscosity of the milled products, played a critical role in the ball milling process. Improper amounts of surfactants and solvent will increase the Fe contamination and decrease the milling efficiency. Besides the grinding time, the size distribution of the milled product has also been found to be closely related with the size of the balls. In addition, other parameters such as the weight ratio of ball to powder also need to be systematically considered to reach high nanoparticle yield, low contamination and the desired size distribution. In our experiments, the typical milling duration used was 20 h with balls of 1/4 inch in diameter. The weight ratio of powder to ball was set as 1:10. The amount of surfactant used was ~8%–10% and the solvent used was about 55% of the weight of the starting powder, respectively. The ground slurry was then dispersed into heptane solvent by ultrasonic vibration and transferred to a 50 ml centrifugal tube for size selection.

The surfactants used are absorbed by the fresh surface of particles crushed during the ball milling, leading to a surface modification for the ground particles. Experimental results show that the function of the surfactants is multifold:

- (1) The surfactants prevent the re-welding of the crushed particles during the ball milling; thus fine particle size can be obtained. Figure 1(a) exhibits a TEM image of the  $\text{Sm}_2\text{Co}_{17}$  sample ground for 20 h. The as-milled particles show irregular shapes and a wide size distribution from several nanometers to larger than 50 nm, indicating that ball milling is effective in reducing the particle size which leads to increased yield of the nanoparticles.
- (2) The surfactant-induced surface modification can greatly enhance the dispersion of  $\text{Sm}_2\text{Co}_{17}$  and  $\text{SmCo}_5$  nanoparticles in a solvent. In our experiments, it was found that the suspending time of these particles ground without surfactants in the solution was less than 1 min, while particles ground with surfactants can be floating in heptane solvent from several tens of seconds to several hours or even many days, depending on the particle size. This size-dependent suspending time provides good opportunities for size selection of the nanoparticles, as we will be discussing later.
- (3) The oil-like surfactants coated on the surfaces also act as lubricants on the particle surfaces, which reduces contamination. The Fe contamination has been estimated by measuring the ball weight loss upon milling and it was found that the weight loss of the balls is less than 0.2% after 20 h ball milling when optimized amounts of surfactants and heptane were used.

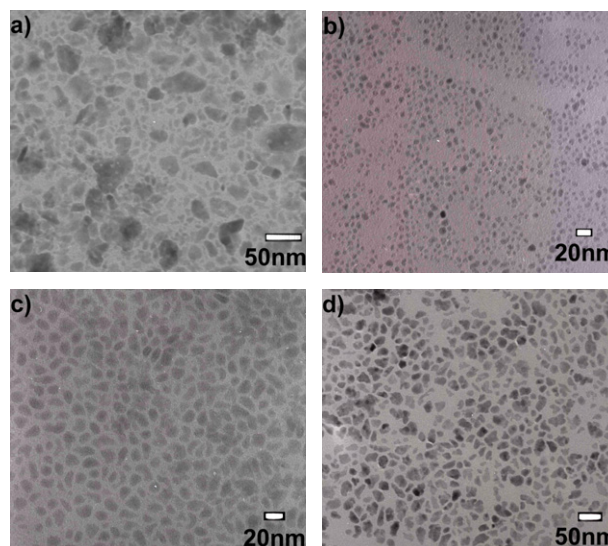


**Figure 1.** TEM images of  $\text{Sm}_2\text{Co}_{17}$  nanoparticles ground for 20 h in heptane with surfactants: (a) the as-milled nanoparticles with sizes about 4–50 nm, (b) nanoparticles separated by centrifugal separation, (c) nanoparticles separated by 2–5 h settling-down time, (d) nanoparticles separated after 20–30 min settling-down time.

Based on the above observations, different sizes of the nanoparticles were separated by using centrifugal separation and controlling the ‘settling-down’ time of the nanoparticle solutions. It was found that the small size nanoparticles are floating in the heptane solvent even after a centrifugation of 3000 rotations per minute (rpm) (relative centrifugal force: 1600g) for 25 min. Therefore, the small nanoparticles can be separated simply by applying a centrifugation procedure to remove large particles from the solution. Figure 1(b) shows the morphology of the nanoparticles with average size of 6 nm obtained from centrifugation of a slurry. To obtain larger nanoparticles, the slurry was washed once by heptane to remove the smallest floating nanoparticles. Then the remaining part was transferred into a surfactant-coated centrifugal tube and dispersed in heptane again by ultrasonic vibration; the dispersed solution was then settled down statically for 2–5 h: we called this the ‘settling-down’ time. After this settling-down time, a low-speed centrifugal separation of 500 rpm (45 g relative centrifugal force) was done to remove the largest particles. The morphology of the nanoparticles that remained after the settling-down process is shown in figure 2(c), where nanoparticles with average size of 13 nm were obtained. Using a similar process but a shorter settling-down time (20–30 min), larger size nanoparticles can be obtained. Figure 1(d) displays the typical morphology of those relatively large nanoparticles (average size 23 nm) separated with 20–30 min settling-down time. Figure 2 gives the statistical size distributions of the nanoparticles after the size-selection process. The charts 1, 2 and 3 correspond to the nanoparticles shown in figures 1(b), (c) and (d), respectively. Compared with the as-milled particles (figure 1(a)), the nanoparticles after the size selection have much more narrow size distributions.

X-ray diffraction patterns of  $\text{Sm}_2\text{Co}_{17}$  nanoparticles of different sizes obtained by the size-selection process are shown

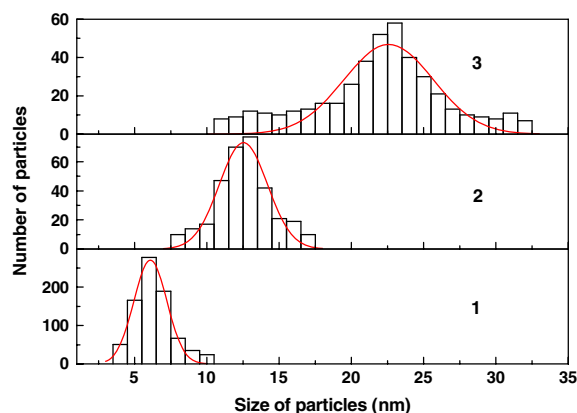


**Figure 2.** The statistical size distributions of the selected nanoparticles. The charts 1, 2, and 3 correspond to the nanoparticles shown in figures 1(b), (c) and (d), respectively.

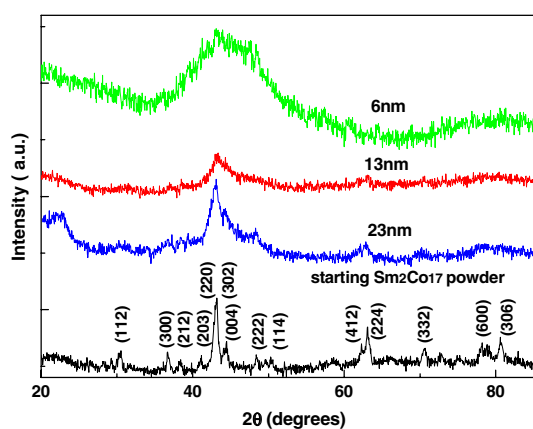


**Figure 3.** X-ray scans of the ball-milled  $\text{Sm}_2\text{Co}_{17}$  samples. No secondary phases are detected from the diffraction patterns and the peaks show obvious broadening with the decreasing particle size.

in figure 3. The pattern of the starting powder is also shown for comparison. It can be seen that no peaks from oxides, pure iron and cobalt are presented in the diffraction patterns, indicating that the prepared nanoparticles have been effectively protected from oxidation by handling the solution in the glove box and embedding the particles in epoxy. Our further experiments proved that  $\text{SiO}_2$  coating improves the oxidation resistance of the ground Sm–Co nanoparticles in air. The diffraction patterns also confirm that no detectable contamination or decomposition in the particles has occurred. The EDX measurements showed that the compositions of the nanoparticle samples were close to the compositions of the starting  $\text{Sm}_2\text{Co}_{17}$  powder. The results also show that the diffraction peaks are broadened with the decreasing particle size, as expected. The strains and amorphization induced by high-energy ball milling may also contribute to the broadening of the diffraction peaks, so it is difficult to quantitatively calculate the particle size from the width of diffraction peaks.

Figure 4 presents the magnetization loops of the  $\text{Sm}_2\text{Co}_{17}$  nanoparticles with different sizes. All the loops show a single-phase-like magnetization behavior (no kinks on the

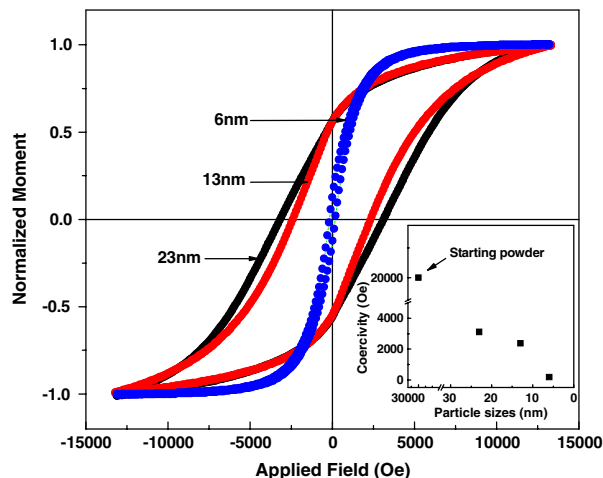


**Figure 4.** Room-temperature magnetization loops of the ball-milled  $\text{Sm}_2\text{Co}_{17}$  nanoparticles. The inset shows the particle size-dependent coercivity of the nanoparticle samples. The particles with average size of 23, 13, and 6 nm have the coercivity of 3.1, 2.4 and 170 Oe, respectively.

demagnetization curves), indicating no second phases in the particles. The inset in figure 4 shows the size-dependent coercivity of the particles. The starting powder, 23 nm, 13 nm and 6 nm samples have coercivity of 20 kOe, 3.1 kOe, 2.4 kOe and 170 Oe at room temperature, respectively. These values are significantly higher compared to the reported values of Sm–Co nanoparticles synthesized by other methods. There is still much to be further understood about the size-dependent coercivity in these nanoparticles. One possible explanation is that increased defects in the smaller particles lower the magnetocrystalline anisotropy [15]. In addition, local strains can also cause low-energy nucleation sites [16, 17]. It is also possible that the ball milling has led to partial amorphization in the nanoparticles and the smaller particles have more amorphous structure which leads to reduced coercivity. Though the quantitative determination of the magnetization values is difficult at present because of the effect of epoxy and surfactants that cover the particles, magnetic measurements have shown decreased saturation magnetization ( $M_s$ ) of the ball-milled nanoparticles with respect to the bulk which may result from size reduction, amorphization and contamination. The 6 nm particles are more reactive and prone to oxidation, which may also result in a loss of magnetocrystalline anisotropy. Further investigation on heat treatments and the detailed particle crystal structure of the ball-milled nanoparticles is underway.

#### 4. Conclusions

In conclusion, Sm–Co nanoparticles with room-temperature ferromagnetism have been successfully produced by surfactant-assisted ball milling. The surfactants used could greatly enhance the dispersion of the nanoparticles in the nanoparticle solutions. A size-selection process based on the improved dispersion has been developed and nanoparticles with different sizes and narrow size distributions were obtained. The

Sm<sub>2</sub>Co<sub>17</sub> nanoparticles with average size of 23 nm have a coercivity value of 3.1 kOe at room temperature. The described surfactant-assisted ball milling and size-selection processes are promising for fabrication of nanoparticles of other rare-earth-containing magnetic materials (e.g., Nd<sub>2</sub>Fe<sub>14</sub>B nanoparticles) and can be developed to be a versatile technique of nanoparticle preparation for other materials in general.

### Acknowledgments

This work is financially supported by ONR/MURI under Grant No N00014-05-1-0497. The authors would like to express appreciations to Dr Jinfang Liu of Electron Energy Corp. for providing the SmCo alloy powders and Dr Jiechao Jiang in the Materials Science and Engineering Department of The University of Texas at Arlington for assistance in TEM observation.

### References

- [1] Sun S, Murray C B, Weller D, Folks L and Moser A 2000 *Science* **287** 1989
- [2] Zeng H, Li J, Liu J P, Wang Z L and Sun S 2002 *Nature* **420** 395
- [3] Strnat K J 1988 *Ferromagnetic Materials* vol 4, ed E P Wohlfarth and K H J Buschow (Amsterdam: North-Holland) pp 131–209
- [4] Ono K, Kakefuda Y, Okuda R, Ishii Y, Kamimura S, Kitamura A and Oshima M 2002 *J. Appl. Phys.* **91** 8480
- [5] Gu H, Xu B, Rao J, Zheng R K, Zhang X X, Fung K K and Wong C Y C 2003 *J. Appl. Phys.* **93** 7589
- [6] Stoyanov S, Skumryev V, Zhang Y, Huang Y, Hadjipanayis G and Noguees J 2003 *J. Appl. Phys.* **93** 7592
- [7] Teng X and Yang H 2007 *J. Nanosci. Nanotechnol.* **7** 356
- [8] Hong J H, Kim W S, Li J I and Hur N H 2007 *Solid State Commun.* **141** 541
- [9] Suryanarayana C 2004 *Mechanical Alloying and Milling* (New York: Dekker)
- [10] Papell S S 1965 *US Patent Specification* 3,215,572
- [11] Kaczmarek W A, Bramley R, Calka A and Ninham B W 1990 *IEEE Trans. Magn.* **26** 1840
- [12] Kirkpatrick E M, Majetich S A and Mchenry M E 1996 *IEEE Trans. Magn.* **32** 4502
- [13] Cha H G, Kim Y H, Kim C W, Kwon H W and Kang Y S 2007 *J. Phys. Chem. C* **111** 1219
- [14] Chakka V M, Altuncevahir B, Jin Z Q, Li Y and Liu J P 2006 *J. Appl. Phys.* **99** 08E912
- [15] Wernick J H 1972 *Annu. Rev. Mater. Sci.* **2** 607
- [16] Shimada Y and Kojima H 1973 *J. Appl. Phys.* **44** 5125
- [17] Chowdary K M, Giri A K, Pellerin K, Majetich S A and Scott J H J 1999 *J. Appl. Phys.* **85** 4331